

Disturbance Compensation for DC Motor Mechanism Low Speed Regulation : A Feedforward and Feedback Implementation

Wei Wu

Abstract—The disturbance torque in the DC motor drive of a scan unit was calculated using the known voltage input to the motor and the measured motor speed response. The cogging torque of the motor and the friction in the mechanism can then be estimated from the calculated disturbance torque. The calculated disturbance torque was further utilized to reduce the speed ripples in speed regulation applications. A combined feedforward and feedback configuration was used to reject the disturbance based on both the off-line calculated disturbance and the on-line estimated disturbance. This scheme was successfully implemented in commercial scan devices. Data obtained under real operating conditions demonstrated the effectiveness and robustness of this disturbance compensation scheme.

I. INTRODUCTION

DC motors are widely used in industrial control systems because they are well understood and easy to control. Usually, the cogging torque, commutation torque, and friction exist in DC motors, causing torque ripples in the motor output torque. For cost reduction reasons, cheaper DC motors are used more in a lot of commercial products such as scanners. For cheap DC motors, these disturbance torques can be quite large, causing performance issues, e.g. speed ripples. Usually, the closed and/or open-loop control are used to suppress the disturbances. In speed regulation applications, conventional industrial proportional, integral, and derivative (PID) controllers may not be very effective in eliminating the speed ripples of motors with small inertia, due to the periodic nature of the disturbance torque. In this case, the disturbance compensation is desirable [2], [1], [5], [3], [4], and [6]. A feed-forward approach is used to compute the disturbances off-line, then save them in a look-up table. Each time the control loop is updated, the controller output is calculated based on a value in the look-up table. This approach needs information of the absolute position of the motor shaft because the disturbance torque could be position dependent, such as the cogging torque. However, this approach may not be robust due to the large variations in motor parameters from motor to motor, especially for cheaper DC motors, as well as the variations in the operating condition of the motor driven mechanisms, such as friction. Therefore, a feedback compensation is desirable besides a feedforward compensation.

Here, we consider compensating the torque disturbance in a closed-loop DC motor speed regulation system. In this type of systems with a PID type controller, speed ripples are typically present in the speed outputs, and the performance gets worse at lower speeds. Besides using the information of the disturbance obtained off-line, an on-line disturbance compensation scheme is also proposed to eliminate the speed ripples at low speeds, thus resulting in a combined feedforward and feedback disturbance compensation structure. This approach can be applied readily to

Senior Control System Engineer, Lexmark International, Lexington, KY, 40550, USA wu_esi@yahoo.com

any existing DC motor closed or open-loop speed regulation system. In this approach, first the disturbance torque is computed off-line using the physical model of the DC motor, based on which a fixed voltage is generated as the feedforward control signal; then, for the feedforward compensated motor drive, the uncanceled disturbance torque is computed on-line, at fixed sampling rate, to generate, via a simple control law, an additional voltage signal in the feedback path to counteract the effect of the uncanceled disturbance torque on the speed output.

This approach does not require any extra sensing. It needs the information on the motor terminal voltage and the motor speed, which is usually available for a closed-loop speed regulation system. The discrete form makes it suitable for direct digital implementation. The effectiveness of the approach was proved through extensive experiments on prototype units. Experimental results demonstrate that the speed performances have been largely improved using the proposed disturbance compensation.

II. OFF-LINE DISTURBANCE COMPUTATION AND COMPENSATION

A. Off-line Disturbance Computation

Consider the following DC motor governing equations

$$L \frac{di}{dt} + iR + k_b \omega = V_T \quad (1)$$

and

$$J \dot{\omega} = k_t i - T_d, \quad (2)$$

where L is the winding inductance, R is the winding resistance, J is the total inertia including the motor inertia and the reflected inertia on the motor shaft of the load, k_b is the back-EMF constant, k_t is the motor torque constant, ω is the motor speed, V_T is the terminal voltage, i is the current, and T_d is the motor disturbance.

Discretize the above two differential equations using the backward Euler's method to have the difference equation for the motor winding current

$$i(k) = \left(\frac{L}{\Delta t} + R\right)^{-1} \left(\frac{L}{\Delta t} i(k-1) - k_b \omega(k) + V_T(k)\right), \quad (3)$$

where Δt is the time interval/sample period, and k is the step number. The disturbance equation is

$$T_d(k) = k_t i(k) - J \dot{\omega}(k). \quad (4)$$

In practice, with the known terminal voltage to a motor at rest, the speed of the motor measured through an optical encoder, and the acceleration computed using the speed measurement, Eqs. (3) and (4) are used to computer the disturbance with the following initial condition

$$\omega(0) = 0.$$

Here, the motor parameters are assumed known or measured. The disturbance consists of the cogging torque which depends on the rotor angular position and the static and dynamic frictions. The static friction is assumed to be constant on average, and the dynamic friction (viscous damping) is constant for a constant motor speed.

B. Off-line Disturbance Compensation

For motor speed regulation applications, especially at the steady state, the periodical disturbance torque can cause the speed ripples. If the disturbance is known to the controller, a voltage can be applied to the motor to counteract the disturbance, eliminating the torque ripples, thus the speed ripples. To accomplish this, an off-line estimation of the disturbance and a feedforward control law that generates the counteracting voltage may be desired. The discrete time disturbance estimation presented earlier can be applied to calculate the disturbance. Next, we present the feedforward disturbance controller.

The motor speed response is due to the terminal voltage regulated by a controller and the disturbance in the motor. Besides the voltage output of the existing controller in the loop, consider a feedforward voltage at the motor terminal required to cancel off the disturbance effect on the speed, V_{ff} . The speed response is

$$\omega = \frac{\frac{1}{k_b}}{t_e t_m s^2 + t_m s + 1} (V + V_{ff}) - \frac{\frac{t_m t_e s + t_m}{J} T_d}{t_e t_m s^2 + t_m s + 1} T_d, \quad (5)$$

where $t_m = \frac{RJ}{k_b k_t}$ is the mechanical time constant, $t_e = L/R$ is the electrical time constant. Choosing V_{ff} to eliminate the effect of T_d on ω , it renders

$$V_{ff}(s) = \frac{t_m k_b}{J} (t_e s + 1) T_d(s), \quad (6)$$

or, in original motor parameters,

$$V_{ff}(s) = \left(\frac{L}{k_t} s + \frac{R}{k_t} \right) T_d(s). \quad (7)$$

Add the disturbance compensating voltage, the overall terminal voltage V_T is

$$V_T = V + V_{ff}, \quad (8)$$

where V is the output of the existing controller. Now, we consider the implementation of the compensation scheme in digital form. Eq. (7) can be discretized using the Euler's method to have

$$V_{ff}(k) = \left(\frac{L}{k_t \Delta t} + \frac{R}{k_t} \right) T_d(k) - \frac{L}{k_t \Delta t} T_d(k-1). \quad (9)$$

$V_{ff}(k)$ can be computed if $T_d(k)$ is known, i.e. given by Eq.(4).

III. ON-LINE DISTURBANCE COMPENSATION SCHEME

We have presented an off-line disturbance torque calculation approach and a feedforward control law. However, since the torque is calculated *a priori*, it can not represent the actual disturbance torque in a real operation due to changes in system parameters and operating conditions. Also, any unexpected disturbances that occur in an operation will not be accounted for. For these reasons, we would like to develop a feedback compensation approach based on the equations we have derived so far.

According to the previous results,

$$i(k) = \left(\frac{L}{\Delta t} + R \right)^{-1} \left(\frac{L}{\Delta t} i(k-1) - k_b \omega(k) + V_T(k) \right), \quad (10)$$

$$T_d(k) = k_t i(k) - J \dot{\omega}(k). \quad (11)$$

Eqs. (9), (10), and (11) are used together to generate the disturbance compensating voltage on-line. At each feedback loop updating time instance, k , $V_{ff}(k)$ is to be generated. According to Eq. (10), $V_T(k)$ needs to be known in order to compute $V_{ff}(k)$, which is not feasible because $V_T(k)$ is not known since $V_{ff}(k)$ is unknown according to Eq. (8). To overcome this problem, we propose to compute $V_{ff}(k)$ in the following way. At step k , $\omega(k-1)$ and $V_T(k-1)$ are known, so $i(k-1)$ can be computed according to Eq. (10). Then, $T_d(k-1)$ can be computed based on Eq. (11). Similarly, $T_d(k-2)$ is obtained. $T_d(k)$ is approximated using linear extrapolation as

$$T_d(k) \approx 2T_d(k-1) - T_d(k-2). \quad (12)$$

Eq. (9) then becomes

$$V_{ff}(k) = \left(\frac{L}{k_t \Delta t} + \frac{2R}{k_t} \right) T_d(k-1) - \left(\frac{L}{k_t \Delta t} + \frac{R}{k_t} \right) T_d(k-2). \quad (13)$$

Finally, Eq. (8) gives $V_T(k)$ for step k .

A. Stability and performance

The disturbance control presented assumes the knowledge of the motor parameters, e.g. the winding inductance and resistance L and R . In reality, the true values of these parameters may not be known or is changing with operating conditions. Because of the feedback nature of this method, the closed-loop may be unstable, if there are significant uncertainties in these parameters. In order to prevent against the instability in the local loop, let

$$\begin{aligned} \tilde{V}_{ff}(k) = & k_r \left[\left(\frac{\hat{L}}{k_t \Delta t} + \frac{2\hat{R}}{k_t} \right) T_d(k-1) - \left(\frac{\hat{L}}{k_t \Delta t} + \right. \right. \\ & \left. \left. + \frac{\hat{R}}{k_t} \right) T_d(k-2) \right], \end{aligned} \quad (14)$$

where \hat{L} , \hat{k}_t , \hat{R} are nominal motor parameters used in calculation, and $0 \leq k_r < 1$ is the stability gain. And, the total terminal voltage implemented is

$$V_T(k) = V(k) + \tilde{V}_{ff}(k), \quad (15)$$

Taking the Z transform of Eq. (10), we have

$$I(z) = \frac{\left(\frac{\hat{L}}{\Delta t} + \hat{R} \right)^{-1}}{1 - \left(\frac{\hat{L}}{\Delta t} + \hat{R} \right)^{-1} \frac{\hat{L}}{\Delta t} z^{-1}} \left(-\hat{k}_b \Omega(z) + V_T(z) \right). \quad (16)$$

Let $\dot{\omega}(k) = \frac{\omega(k) - \omega(k-1)}{\Delta t}$ in Eq. (11) and take the Z transform of Eq. (11), we have

$$\begin{aligned} T_d(z) = & \frac{\alpha_1 + \alpha_2 z^{-1} + \alpha_3 z^{-2}}{1 - \left(\frac{\hat{L}}{\Delta t} + \hat{R} \right)^{-1} \frac{\hat{L}}{\Delta t} z^{-1}} \Omega(z) + \\ & + \frac{\hat{k}_t \left(\frac{\hat{L}}{\Delta t} + \hat{R} \right)^{-1}}{1 - \left(\frac{\hat{L}}{\Delta t} + \hat{R} \right)^{-1} \frac{\hat{L}}{\Delta t} z^{-1}} V_T(z), \end{aligned} \quad (17)$$

where $\alpha_1, \alpha_2, \alpha_3$ are in the Appendix. Based on the Z transform of Eq. (14),

$$\tilde{V}_{ff}(z) = k_r \left[\left(\frac{\hat{L}}{k_t \Delta t} + \frac{2\hat{R}}{k_t} \right) z^{-1} - \left(\frac{\hat{L}}{k_t \Delta t} + \frac{\hat{R}}{k_t} \right) z^{-2} \right] T_d(z), \quad (18)$$

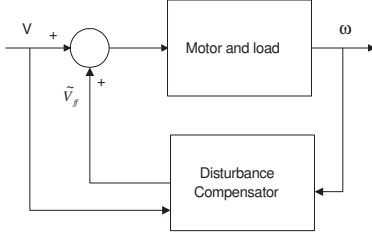


Fig. 1. Local loop

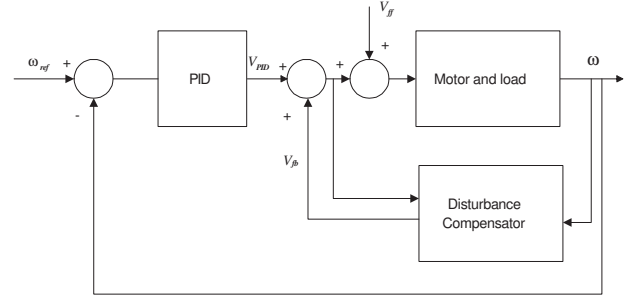


Fig. 2. Combined feedforward and feedback structure

we have

$$\begin{aligned} \tilde{V}_{ff}(z) = & k_r \frac{\beta_1 z^{-1} + \beta_2 z^{-2} + \beta_3 z^{-3} + \beta_4 z^{-4}}{1 - (\frac{L}{\Delta t} + \hat{R})^{-1} \left[(1 + k_r) \frac{L}{\Delta t} + 2k_r \hat{R} \right]} \Omega(z) \\ & + k_r \frac{(\frac{L}{\Delta t} + \hat{R})^{-1} (\frac{L}{\Delta t} + 2\hat{R}) z^{-1} - z^{-2}}{1 - (\frac{L}{\Delta t} + \hat{R})^{-1} \left[(1 + k_r) \frac{L}{\Delta t} + 2k_r \hat{R} \right]} V(z), \end{aligned} \quad (19)$$

where $\beta_1, \beta_2, \beta_3, \beta_4$ are in Appendix.

Proposition 1. Consider the closed-loop system, Fig. 1, consisting of the motor,

$$\omega = \frac{1}{k_b} (V + \tilde{V}_{ff}) - \frac{t_m t_e s + t_m}{t_e t_m s^2 + t_m s + 1} T_d, \quad (20)$$

and the disturbance compensator, Eq. 19. Under the parameter uncertainty and unmodelled dynamics in the motor, this loop is stable provided that k_r is sufficiently small.

Proof: For $0 \leq k_r < 1$, the disturbance compensator is stable, i.e. all poles inside the unit circle. k_r can be chosen such that the loop gain is less than unity. According to the Small Gain theorem, the feedback system is stable.

The smaller k_r is, the smaller the disturbance compensation effectiveness. Consider the sampled data system consisting of the motor and the digital disturbance compensator, Fig. 1. The output speed ω is a function of the control voltage V and the motor intrinsic disturbance T_d . From Eq. 20, the DC gain of the motor for control voltage and disturbance is $1/k_b$ and t_m/J , respectively. Under the proposed disturbance compensation, the DC gain for control voltage is unchanged. and the DC gain for disturbance assuming all motor parameters are precisely known, is

$$\frac{1 - (\frac{L}{\Delta t} + R)^{-1} \left[(1 + k_r) \frac{L}{\Delta t} + 2k_r R \right] + k_r t_m}{1 - (\frac{L}{\Delta t} + R)^{-1} \frac{L}{\Delta t}} \frac{1}{J}. \quad (21)$$

This quantity equals zero when $k_r = 1$ and t_m/J when $k_r = 0$. Thus disturbance rejection performance is compromised for robust stability in applications. Also, due to less disturbance effect under the disturbance compensation, for a constant input voltage (V) to the motor, the average motor speed is higher than the average speed under the same input voltage without the disturbance compensation. This higher motor gain increases the loop gain consequently, which may not be desirable for an originally optimal controller. Thus, the gain of the original controller may be lowered to make the loop gain unchanged when implementing this scheme inside a existing control loop.

IV. A COMBINED FEEDFORWARD AND FEEDBACK COMPENSATION IMPLEMENTATION

We have presented a feedforward and feedback disturbance compensation approach, respectively, in the previous sections. It is natural and practical to combined these two approaches together to obtain a combined feedback and feedforward compensation structure, shown in Fig. 2.

The feedforward disturbance compensation is expected to reject most of the disturbance, where V_{ff} in Fig. 2 is calculated using Eq. 9 based on the off-line disturbance torque obtained as in Section 2. For the feedforward compensated motor drive mechanism, there will still be some amount of disturbance left in the system. The feedback on-line disturbance compensation we developed earlier can be subsequently applied around this system to cancel the remaining disturbance in the system, where V_{fb} is computed as \hat{V}_{ff} is in Section 3. This feedback loop around the feedforward compensated motor mechanism provides further performance improvement against these disturbances unaccounted for in the off-line computation.

V. IMPLEMENTATION AND RESULTS

We will first show the off-line disturbance computation and the feedback disturbance compensation of a motor, respectively. Then we will present the application of the combined feedforward plus feedback disturbance compensation to real commercial scan units. Extensive reliability testing conducted on engineering samples and large amount of statistical data collected from the various manufacture lines validated the effectiveness and robustness of this control scheme. These scan units are currently on the consumer markets.

A. DC motor in open loop

We implement our methods to a Mabuchi RK370 motor. The parameters of the motor given in the motor specifications for reference are summarized in Table 1.

TABLE I
MABUCHI MOTOR PARAMETERS

Parameter	Value	Unit
Terminal resistance	$17 \pm 15\%$	Ω
Terminal inductance	N/A	Henry
Torque constant	$18.3 \pm 18\%$	mNm/A
Mass moment of inertia	9.0	gcm^2
Cogging torque	1.86(max.), 1.57 ptp.(max.)	mNm

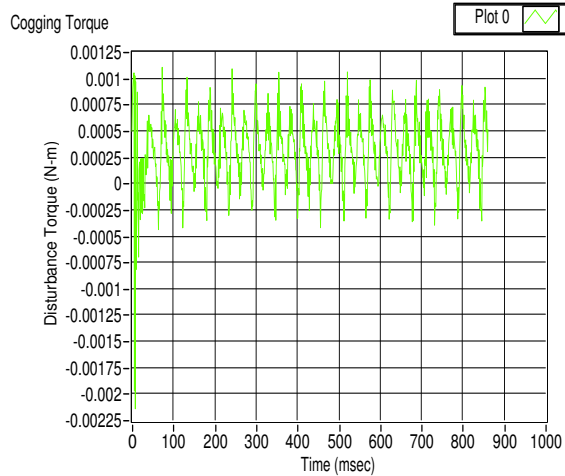


Fig. 3. Disturbance Torque

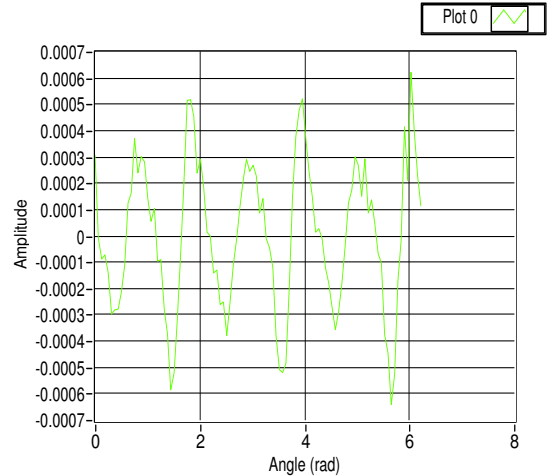


Fig. 4. calculated average cogging torque

Note the inductance is not given by the specifications. The inductance of the motor for experiment was measured as $L = 20.25mH$. Also note the values given in the table is for reference only. A large amount of variations in the parameters exist from motor to motor, e.g. the resistance of the motor under test is $16.4ohm$. To test the robustness of our methods, we use resistance, torque constant, mass moment of inertia in the specifications and the measured inductance for disturbance calculation and compensation.

To calculate the disturbance torque, we sent $2volt$ to the motor PWM driver. We measured motor shaft speed and position using an optical encoder with 448 quadrature counts per revolution(CPR). The speed and angular position of the rotor over five revolutions were measured. The calculated torque versus time is shown in Fig. 3.

Fig. 3 shows that the stiction was broken when the motor started to move from rest. When the rotor was moving, the cogging torque and dynamic friction dominated and the total disturbance appears periodic. To eliminate the transient effect in the calculation of the cogging torque, we calculated the torque for the last four revolutions respectively, then took the average as the disturbance torque. The mean of the disturbance torque over one revolution gives the value of the friction. Removing the mean from the disturbance torque gives the cogging torque. The calculated cogging torque versus the angular position is shown in Fig. 4. And the calculated friction is $0.333mNm$. Fig. 4 shows that the calculated cogging torque is periodic and has peak to peak values in agreement with the specifications, see Table 1.

Next, we applied the on-line disturbance estimation and compensation for motor speed regulation. Speed ripples exist in motor speed due to the existence of the cogging torque. It may be harmful for some speed regulation applications, especially at low speeds. This on-line disturbance compensation scheme was proven to be effective in reducing the speed ripples through experiment. In this experiment, $1volt$ command voltage was sent into the motor driver. The speeds with and without the disturbance cancellation are shown in Fig. 5 and Fig. 6, respectively. The standard deviation of the speed at steady state is $0.022ips$ without compensation, and $0.011ips$ with disturbance cancellation, respectively. A 50%

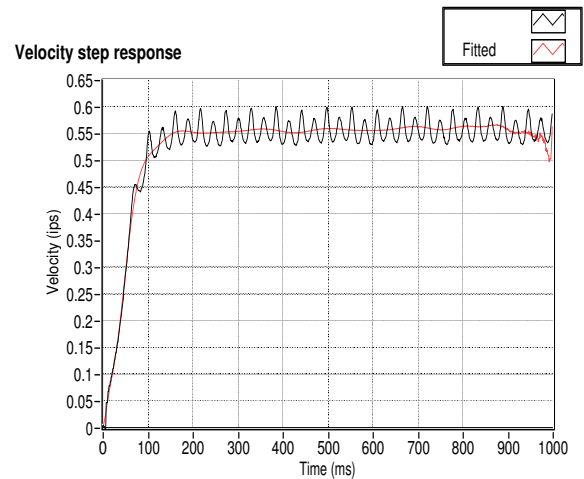


Fig. 5. Speed w/o compensation

improvement was achieved. Also, the steady state speed is faster with compensation because an extra terminal voltage is applied to overcome the friction. The terminal voltage with compensation is shown in Fig. 7.

B. DC motor scan mechanism in PID closed loop

The application of the combined scheme to a closed-loop DC motor system has also been implemented. A DC motor driven mechanism carrying a CIS scan bar in a flatbed scan unit had a proportional, integral and derivative (PID) controller to regulating the scan speed. The mechanism consisted of a pulley, gear, and belt transmission which moves the scan bar. A Mabuchi FC130 motor, which was driven by a pulse-width-modulated(PWM) drive, was used to drive the transmission. A 112 CPR quadrature digital output encoder mounted on the motor shaft was the position and speed sensor. The combined disturbance compensation was implemented in the firmware using integer arithmetic. The control loop updates every one milli-second. For the PID controller in the speed loop, the proportional gain is 5, and the integral gain is 1000, and the

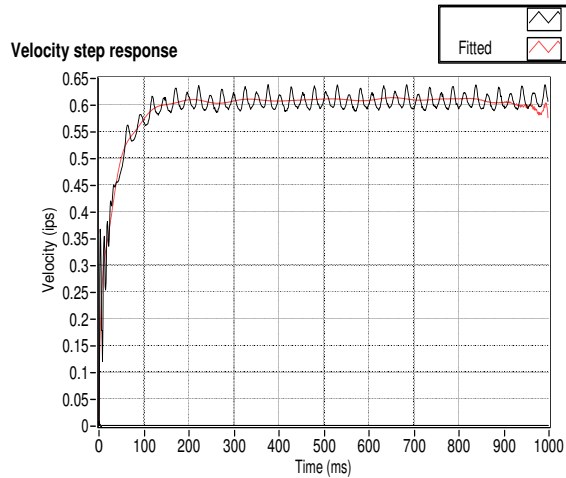


Fig. 6. Speed w/ compensation

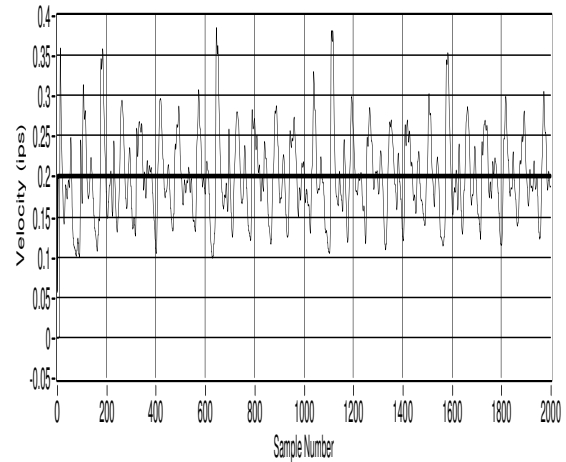


Fig. 8. PID control steady state speed

Terminal voltage

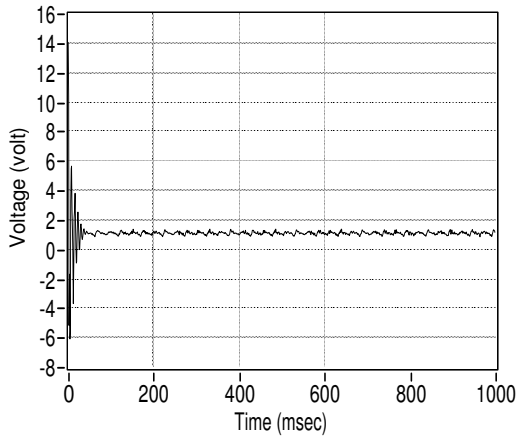


Fig. 7. Motor terminal voltage applied

derivative gain is 5, all in its appropriate unit respectively. For 600 pixel per inch (PPI) scan, the required speed is $0.2ips$. The speed response with the PID controller was shown in Fig. 8, with motor terminal voltage in Fig. 9. From Fig. 8, the speed response was very poor, and the corresponding scan image test failed. Tuning the PID gains has proved to be ineffective in this case after many trials.

The combined strategy was applied to the PID loop. Nominal motor parameter values from the manufacturer's motor specifications were used for the model, and the reflected load inertia on the motor was ignored in purpose. This serves to test the robustness of the proposed scheme. When a scan command is issued, the scanner will first make a short move, return to the home position, then make the actual scan move. The off-line disturbance computation was done based on the collected speed and voltage data after the pre-move, during which the system was controlled by the PID controller. The actual 600ppi(pixel per inch) scan move took place after the pre-move, during which both the feedforward and the feedback disturbance compensation were turned on in addition to the PID

controller. The disturbance torque computed off-line was obtained by averaging over several shaft revolutions and was mapped to the 448 quadrature encoder edges, i.e. see Fig. 4. Note that there are 448 quadrature edges per shaft revolution. The encoder edge counts which increases or decreases during an actual operation which comprises both the pre-move and the scan move, was saved in a register in the ASIC which was reset to zero before every scan operation. At each sample instant, based on the overall counts in the register, the corresponding disturbance torque value at the current shaft position was found. Knowing the current and the previous disturbance torque values, the feedforward voltage can be generated according to Eq. (9). For the feedback disturbance rejection, $k_r = 0.15$ gave the best results in this case through several trials. Based on the experimental results, the feedback disturbance compensation improved the performance of the feedforward compensated PID closed-loop by 10% – 15%. Figure 10 and Fig. 11, shows the speed response and the voltages, respectively, under the combined disturbance compensation scheme. From Fig. 10, it is evident that a significant performance improvement was achieved at steady state. Under the current scheme, there was larger error and more oscillations in the transient responses compared to the PID control. However, in our application, scan occurs only after the speed reaches the steady state. Steady state speed regulation was our focus. Thus, this application of the proposed disturbance compensation scheme for low speed regulation was considered very successful.

VI. CONCLUSIONS

Based on the DC motor equations, the disturbance torque in a mechanism can be computed in either off-line or on-line fashion. Consequently, control laws are derived to reject the disturbance utilizing the computed disturbance torque. Robust stability condition and performance index are discussed for the on-line disturbance compensation. A combined online and off-line(feedback and feedforward) scheme is proposed. Experimental results proved the effectiveness of the scheme, including a motor example and a real application example of consumer scan units. In both cases, the steady state speed performances were significantly improved.

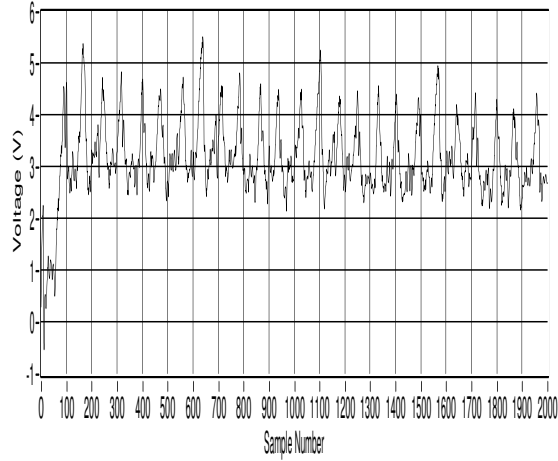


Fig. 9. PID control terminal voltage

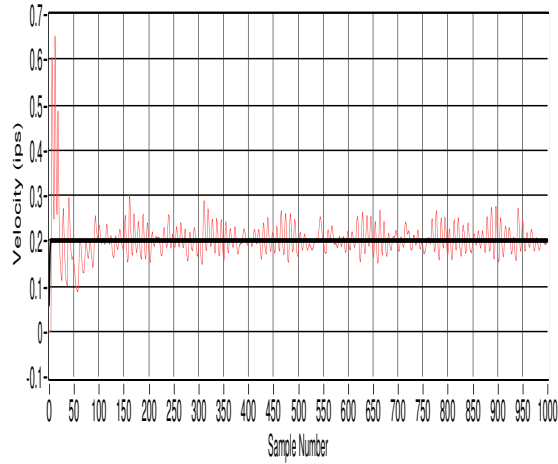


Fig. 10. Speed under the combined scheme: actual speed(thin), reference speed(heavy)

This approach is especially suitable for improving an existing speed regulation system and can be easily implemented in its digital form.

REFERENCES

- [1] Alvarez-Ramirez, J., Femat, R., and Barreiro, A., "A PI Controller with Disturbance Estimation," *Ind. Eng. Chem. Res.*, 36, pp. 3668-3675, 1997.
- [2] Chung, M., and Kang, D., "Nano Positioning System using Trajectory Following Control Method with Cogging Force Model," *The 3rd International Symposium on Nanomanufacturing*, Nov. 3-5, 2005.
- [3] Liu, C., Peng, H., "Disturbance Estimation Based Tracking Control For A Robotic Manipulator," *ACC*, 1997.
- [4] Nuninger, W., Balaud, B., and , Kratz, F., "Disturbance Rejection Using Output and Input Estimation. Application to the Friction Compensation of A DC Motor," *Control Eng. Practice*, Vol. 5, No. 4, pp. 477-483, 1997.
- [5] She, J., Ohyama, Y., "Estimation and Rejection of Disturbances in Servo Systems," *The 15th IFAC World Congress*, July 21-26, 2002.
- [6] Wu, W., "DC Motor Speed Control Improvement via On-line Disturbance Computation and Compensation," *Proceedings of IEEE Conference on Decision and Control*, Shanghai, China, 2009.

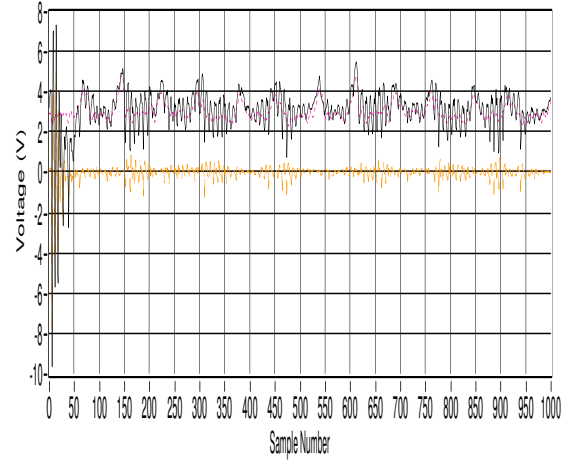


Fig. 11. Voltages under the combined scheme: total voltage(solid), feed-forward disturbance voltage(dashed), feedback disturbance voltage(dash-dotted)

- [7] Xu, Q. and Li, Y., "Dahl Model-based Hysteresis Compensation and Precise Positioning Control of an XY Parallel Micromanipulator with Piezoelectric Actuation," *Journal of Dynamic System, Measurement, and Control*, Vol. 132, July 2010.

APPENDIX

$$\alpha_1 = -k_t k_b \left(\frac{L}{\Delta t} + R \right)^{-1} - \frac{J}{\Delta t} \quad (22)$$

$$\alpha_2 = \frac{JL}{\Delta t^2} \left(\frac{L}{\Delta t} + R \right)^{-1} + \frac{J}{\Delta t} \quad (23)$$

$$\alpha_3 = -\frac{JL}{\Delta t^2} \left(\frac{L}{\Delta t} + R \right)^{-1} \quad (24)$$

$$\beta_1 = -\frac{J}{\Delta t} \left(\frac{L}{k_t \Delta t} + \frac{2R}{k_t} \right) - k_b \left(\frac{L}{\Delta t} + R \right)^{-1} \left(\frac{L}{\Delta t} + 2R \right) \quad (25)$$

$$\beta_2 = k_b + \frac{J}{k_t \Delta t} \left(\frac{2L}{\Delta t} + 3R \right) + \frac{JL}{k_t \Delta t^2} \left(\frac{L}{\Delta t} + R \right)^{-1} \left(\frac{L}{\Delta t} + 2R \right) \quad (26)$$

$$\beta_3 = -\frac{J}{k_t \Delta t} \left(\frac{L}{\Delta t} + R \right) - \frac{JL}{k_t \Delta t^2} \left(\frac{L}{\Delta t} + R \right)^{-1} \left(\frac{2L}{\Delta t} + 3R \right) \quad (27)$$

$$\beta_4 = \frac{JL}{k_t \Delta t^2} \quad (28)$$